Medical Engineering and Physics 38 (2016) 1439–1448

Contents lists available at ScienceDirect

Medical Engineering and Physics

journal homepage: www.elsevier.com/locate/medengphy

A theoretical computerized study for the electrical conductivity of arterial pulsatile blood flow by an elastic tube model

Hua Shen[a,b], Yong Zhu[a], Kai-Rong Qin[a,*]

[a] Department of Biomedical Engineering, Faculty of Electronic Information and Electrical Engineering, Dalian University of Technology, No. 2, Linggong Rd., Dalian 116024, PR China

[b] Department of Electronic Engineering, Dalian Neusoft University of Information, No. 8, Ruanjianyuan Rd., Dalian 116023, PR China

ARTICLE INFO

Article history:
Received 4 February 2016
Revised 25 August 2016
Accepted 23 September 2016

Keywords:
Theoretical modeling
Electrical conductivity
Arterial pulsatile blood flow
Elastic tube
Rigid tube

ABSTRACT

The electrical conductivity of pulsatile blood flow in arteries is an important factor for the application of the electrical impedance measurement system in clinical settings. The electrical conductivity of pulsatile blood flow depends not only on blood-flow-induced *red blood cell* (RBC) orientation and deformation but also on artery wall motion. Numerous studies have investigated the conductivity of pulsatile blood based on a rigid tube model, in which the effects of wall motion on blood conductivity are not considered. In this study, integrating Ling and Atabek's local flow theory and Maxwell–Fricke theory, we develop an elastic tube model to explore the effects of wall motion as well as blood flow velocity on blood conductivity. The simulation results suggest that wall motion, rather than blood flow velocity, is the primary factor that affects the conductivity of flowing blood in arteries.

1. Introduction

Over the past few decades, a number of investigations have demonstrated that the electrical conductivity of pulsatile blood flow in arteries is an important player for electrical impedance measurement system applications in clinical settings [1,19,21,24,27]. The changes in blood electrical conductivity are reported to mainly result from blood-flow-induced orientation and deformation of *red blood cells* (RBCs) [6,8,18,22]. In addition, it has been demonstrated that the characteristics of blood flow, e.g., steady flow or pulsatile flow in the artery, are critical in determining the electrical conductivity of arterial blood flow.

The effects of steady flow on the variation in electrical conductivity of blood have been well documented since the 1970s [6,8,18,22]. These researchers found that the change in electrical conductivity is primarily influenced by the orientation and deformation of RBCs; both are determined by fluid shear stress during steady flow [13,23]. Then, Gaw et al. [9–11] first reported the impact of pulsatile blood flow on electrical conductivity in a straight rigid model using the Womersley theory [28]. This study also found that the variation in electrical conductivity is affected by RBC orientation and deformation. The deformation of RBCs is determined by shear stress, while the orientation ratio of RBCs is determined by the shear rate during pulsatile flow.

It should be noted that all of these previous investigations were based on the assumption that the arterial wall is rigid [9–11,13,17,23]; however, this is not true under physiological conditions. In in vivo arteries, arterial walls undergo elastic deformations. The interaction between wall motion and pulsatile blood flow may lead to significant nonlinear effects on pulsatile blood flow and shear stress [2,4,14,15,25,26,29]; this interaction definitely influences RBC orientation and deformation, thus changing arterial electrical conductivity. However, to date, the quantitative relationship between electrical conductivity, wall motion, and pulsatile blood flow dynamics still remains elusive.

In this paper, we attempt to explore the relationship between electrical conductivity, wall motion, and pulsatile blood flow dynamics by proposing an elastic tube model and analyzing the effect of wall motion on pulsatile blood flow and arterial pulsatile blood flow conductivity. The elastic tube model integrates Ling and Atabek's 'local flow theory' [15] and the Maxwell–Fricke theory [7] and focuses on the orientation and deformation of ellipsoidal particles induced by shear stresses [9–11,13]. Moreover, particular attention is paid to clarifying the contribution of the arterial radius as well as the axial center-line velocity to blood conductivity; these can easily be measured by the Doppler ultrasonic technique [16].

2. Proposed elastic tube model

This section first presents a proposed elastic tube model for the electrical conductivity of arterial pulsatile blood flow. Then, we model the conductivity changes as functions of wall motion,

* Corresponding author.
E-mail address: krqin@dlut.edu.cn (K.-R. Qin).

http://dx.doi.org/10.1016/j.medengphy.2016.09.013
1350-4533/

blood-flow-induced RBC orientation and deformation and finally give the equations and numerical simulation methods.

2.1. Elastic tube model and equations

2.1.1. Pulsatile blood flow dynamics

Pulsatile blood flow in a straight and circular artery can be modeled as a homogeneous, incompressible Newtonian fluid flow in an isotropic, thin-walled, elastic tube with a longitudinal constraint. The continuity and Navier–Stokes equations governing pulsatile blood flow can be simplified as follows [2,15,25,28]

$$\frac{\partial u}{\partial t}+u\frac{\partial u}{\partial x}+v\frac{\partial u}{\partial r}=-\frac{1}{\rho}\cdot\frac{\partial p}{\partial x}+\frac{\eta}{\rho}\cdot\left(\frac{\partial^2 u}{\partial r^2}+\frac{1}{r}\cdot\frac{\partial u}{\partial r}\right) \tag{1}$$

$$\frac{\partial u}{\partial x}+\frac{1}{r}\cdot\frac{\partial(rv)}{\partial r}=0 \tag{2}$$

with boundary conditions of

$$\left.\frac{\partial u}{\partial r}\right|_{r=0}=0,\ v|_{r=0}=0 \tag{3}$$

$$u|_{r=R}=0,\ v|_{r=R}=\frac{\partial R}{\partial t} \tag{4}$$

where u and v denote the axial velocity and radial velocity, respectively; p is blood pressure; ρ and η denote the density and viscosity of blood, respectively; t is a symbol of time; x and r are the longitudinal and radial coordinates, respectively; and R is the arterial inner radius.

By introducing a relative radial coordinate $y=r/R$ into Eq. (1), the axial velocity in the straight artery has the following radial distribution

$$\frac{\partial u}{\partial t}=-\frac{1}{\rho}\cdot\frac{\partial p}{\partial x}+\frac{\eta}{\rho}\cdot\frac{1}{R^2}\cdot\left(\frac{\partial^2 u}{\partial y^2}+\frac{1}{y}\cdot\frac{\partial u}{\partial y}\right)+\frac{1}{R}\cdot\frac{\partial u}{\partial y}\cdot\left(y\cdot\frac{\partial R}{\partial t}-v\right)+\frac{u}{R\cdot y}\cdot\left(v+y\cdot\frac{\partial v}{\partial y}\right) \tag{5}$$

Let us introduce Ling and Atabek's 'local flow theory' [15], that is, assuming that a small variation in x does not change the shape of the axial velocity profiles, the longitudinal gradient of the axial velocity u satisfies:

$$\frac{\partial u}{\partial x}=f(x,t)\cdot|u(x,y,t)| \tag{6}$$

Thus, by introducing Eq. (6) into Eq. (2), the radial velocity can be expressed as follows:

$$v=\frac{\partial R}{\partial x}\cdot\left(yu-\frac{2}{y}\cdot\int_0^y yudy\right)-\frac{R}{y}\cdot f(x,t)\cdot\int_0^y y|u|dy \tag{7}$$

In Eq. (7), $\frac{\partial R}{\partial x}$ can be expressed by

$$\frac{\partial R}{\partial x}=\left(\frac{\partial R}{\partial p}\right)\cdot\left(\frac{\partial p}{\partial x}\right) \tag{8}$$

where $\frac{\partial R}{\partial p}$ is determined by the arterial elastic properties and geometry of the arterial partial zero-stress state that can be measured by the pressure waveform $p(t)$ and radius waveform $R(t)$ using a Doppler ultrasonic instrument.

The pressure gradient can be derived from Eqs. (5)–(8), as follows [5]:

$$\frac{\partial p}{\partial x}=\frac{-\frac{\partial u_c}{\partial t}+\frac{u_c\cdot|u_c|}{R\cdot\int_0^1 y|u_c|dy}\cdot\left(\frac{\partial R}{\partial t}\right)+\frac{2}{R^2}\cdot\frac{\eta}{\rho}\cdot\left(\frac{\partial^2 u_c}{\partial y^2}\right)_{y=0}}{\frac{1}{\rho}-2\cdot\frac{\partial R}{\partial p}\cdot\frac{u_c}{R}\cdot\frac{\int_0^1 yudy}{y|u_c|}\cdot u_c} \tag{9}$$

where u_c is the center-line blood velocity at $y=0$.

The radial velocity v can be deduced from Eqs. (7)–(9), as follows:

$$v=\frac{\partial R}{\partial p}\cdot\frac{\partial p}{\partial x}\left[yu-\frac{2}{y}\cdot\left(\int_0^y yudy\right)-\frac{\int_0^1 yudy}{\int_0^1 y|u|dy}\cdot\int_0^y y|u|dy\right]+\frac{1}{y}\cdot\frac{\partial R}{\partial t}\cdot\frac{\int_0^y y|u|dy}{\int_0^1 y|u|dy} \tag{10}$$

The axial velocity u and radial velocity v can be deduced from Eqs. (5), (9) and (10). Then, the axial shear stress τ_{rx} and radial shear stress τ_{rr} are expressed as:

$$\tau_{rx}=\frac{\eta}{R}\cdot\frac{\partial u}{\partial y} \tag{11}$$

$$\tau_{rr}=2\cdot\frac{\eta}{R}\cdot\frac{\partial v}{\partial y} \tag{12}$$

Because the radial shear stress τ_{rr} is far smaller than the axial shear stress τ_{rx}, i.e., $\tau_{rr}<<\tau_{rx}$, the total shear stress τ at time t is approximated as:

$$\tau\approx\tau_{rx}=\frac{\eta}{R}\cdot\frac{\partial u}{\partial y} \tag{13}$$

For the special case when wall motion is ignored, the elastic tube model is degenerated as a rigid tube model. The shear stress τ_{rg} in the rigid tube model is then expressed as follows (after [16]):

$$\tau_{rg}(y,t)=\frac{\eta}{\bar{R}}\sum_{n=-\infty}^{+\infty}\frac{\alpha_n j^{\frac{3}{2}}J_1(\alpha_n j^{\frac{3}{2}}y)}{J_0(\alpha_n j^{\frac{3}{2}})-1}u(0,\omega_n)e^{j\omega_n t} \tag{14}$$

where n is the harmonic number; J_0 and J_1 are the 0th-order and 1th-order Bessel functions of the first kind, respectively; $j=\sqrt{-1}$; $\bar{R}$ is the time-averaged arterial inner radius over one cardiac cycle; $\alpha_n=\bar{R}\sqrt{\rho\omega_n/\eta}$ is the Womersley number; $\omega_n=2n\pi f$ is the angular frequency; f is the base frequency; and $u(0,\omega_n)$ is the nth harmonic component of the measured center-line velocity $u_c(t)$ and satisfies

$$u_c(t)=\sum_{n=-\infty}^{+\infty}u(0,\omega_n)e^{j\omega_n t} \tag{15}$$

Eqs. (14) and (15) describe the relationship between the shear stress τ_{rg} and center-line velocity $u_c(t)$ in the rigid tube model. Once the center-line velocity $u_c(t)$ and time-averaged radius $\bar{R}$ are given, the frequency components $u(0,\omega_n)$ of $u_c(t)$ are calculated by Eq. (15), and the shear stress τ_{rg} is then calculated using Eq. (14).

2.1.2. Conductivity of blood

In this study, flowing blood with insulating RBCs is modeled as a flowing insulating suspension with ellipsoidal particles. The bulk conductivity $\sigma_{bl}(t)$ of flowing blood is calculated as follows (after [11,13]):

$$\sigma_{bl}(t)=\frac{2}{\bar{R}^2}\cdot\int_0^{\bar{R}}\sigma_c(r,t)rdr \tag{16}$$

where $\sigma_c(r,t)$ is the conductivity of blood at any radial coordinate r that can be calculated by the Maxwell–Fricke Eq. [7]:

$$\frac{\sigma_c}{\sigma_p}=\frac{1-H}{1+(C-1)\cdot H} \tag{17}$$

where σ_p is the conductivity of the plasma; H is the haematocrit expressed as the volume fraction of RBCs relative to the total blood volume; and C is a factor that depends on the geometry and orientation of the RBC and is affected by shear stress.

The expressions for factor C can be found in the literature [3,11,13]. For an easy reference, these expressions are also presented as follows:

$$C=f(r)\cdot C_b+(1-f(r))\cdot C_r \tag{18}$$

Table 1
Values of the model parameters used in numerical simulation.

Parameter	Value	Description	Reference
H	0.45	Haematocrit of whole blood	[11]
ρ	1.05 g/cm^3	Density of blood	[11]
η_{pl}	0.0135 Poise	Viscosity of plasma	[11]
η_{bl}	$\eta_{pl}(1+2.5H+0.0737H)$	Viscosity of whole blood	[11]
λ	1.5×10^{-5} N/m	Membrane shear modulus of cell	[11]
$a_{0/}b_0$	0.38	The ratio of short to long axes of the cell	[13]
b_0	4 μm	Major axis length of RBC	[11]
σ_p	1.12 S/m	Conductivity of the plasma	[11]

$$C_r = \frac{1}{3}(C_a + 2\cdot C_b) \tag{19}$$

$$C_a = \frac{1}{M} \tag{20}$$

$$C_b = \frac{2}{2-M} \tag{21}$$

$$M(a<b) = \frac{\phi - \frac{1}{2}\sin(2\phi)}{\sin^3(\phi)}\cdot\cos(\phi) \tag{22}$$

$$\cos(\varphi) = \frac{a}{b} \tag{23}$$

$$\frac{a}{b} = \frac{a_0}{b_0}\left[1 + \frac{\tau(y,t)\cdot b_0}{4\lambda}\right] \tag{24}$$

$$f(r) = \frac{\tau_o^{-1}(y)}{\tau_d^{-1}(y) + \tau_o^{-1}(y)} \tag{25}$$

$$\tau_o(y) = \left(\frac{1}{R}\frac{du}{dy}\right)^{-1} \tag{26}$$

$$\tau_d(y) = \left(\frac{1}{R}\frac{du}{dy}\right)^{-\frac{1}{2}} \tag{27}$$

In the above expressions, the initial axis lengths of a_0 and b_0 of a RBC is deformed in the presence of a shear stress $\tau(y, t)$; λ is the surface shear modulus of the cell membrane.

2.2. Model parameters and numerical simulation methods

2.2.1. Model parameters

To model the conductivity of pulsatile blood flow in this study, all of the values for the model parameters used in the numerical simulations are listed in Table 1. These values are taken from the literature [11,13]. Unless otherwise specified, these parameters are the default values used throughout the paper.

2.2.2. Numerical simulation method

To quantitatively analyze the relationship among electrical conductivity, wall motion, and pulsatile blood flow dynamics, comparative studies between the elastic tube model and rigid tube model are carried out by numerically simulating the electrical conductivity of pulsatile blood flow. The arterial radius $R(t)$ and center-line velocity u_c(t) used in the numerical simulations are measured in a human common carotid artery (male, 19 years old) by an ultrasound Doppler instrument (ProSound Alpha 7, Aloka), as shown in Fig. 1. Unless otherwise specified, the radius and center-line waveforms shown in Fig. 1 are the default waveforms used throughout the paper.

For the rigid tube model, the shear stress can be directly calculated from Eq. (14). For the elastic tube model, it is assumed that there is a linear relationship between the changes in vessel diameter and changes in blood pressure within each cardiac cycle [20], and the mean value of carotid arterial pressure p_m and diastolic pressure p_d are approximately equal to the mean value of brachial pressure and diastolic pressure, as presented in the literature [12]. Thus, $\frac{\partial R}{\partial p}$ is calculated by

$$\frac{\partial R}{\partial p} = \frac{R_m - R_d}{p_m - p_d}, \tag{28}$$

where p_d and R_d are the diastole blood pressure and corresponding arterial radius, respectively; the mean blood pressure p_m and mean radius R_m are calculated as follows [16]:

$$p_m = p_d + \frac{1}{3}(p_s - p_d), \tag{29}$$

and

$$R_m = \frac{1}{T}\int_0^T R(t)dt, \tag{30}$$

Here, p_s is the systolic blood pressure and T is the period of one cardiac cycle. Finally, the pressure gradient $\partial p/\partial x$ can be numerically calculated by Eq. (9). Once the pressure gradient $\partial p/\partial x$ is obtained, the radial velocity v and axial velocity u can be numerically solved from Eqs. (5), (9) and (10). The shear stress is finally calculated by Eq. (13). In all of the numerical simulations by the elastic tube model, the finite difference schema is adopted as previously published [4,15,26]. After the shear stress is obtained, the conductivity of flowing blood that is affected by shear stress is calculated by Eqs. (16)–(27).

3. Simulation results

This section presents the numerical simulation results for the elastic tube model and/or the rigid tube model.

3.1. Comparison of conductivity between elastic tube model and rigid tube model

Fig. 2 shows the comparison between the simulated conductivity over one cardiac cycle from the elastic tube model and the rigid tube model. It is clearly seen that the pulsating amplitude of the conductivity in the elastic tube model is significantly greater than that in the rigid tube model. To understand how the conductivity changes with arterial radius over one cardiac cycle, the conductivity waveform shown in Fig. 2 and the radius waveform shown in Fig. 1 are presented by conductivity versus radius plotting (Fig. 3).

It is evident from Fig. 3 that the conductivity in the elastic tube model increases as the radius increases during the systolic phase and decreases as the radius decreases during the diastolic phase. These changes occur in an approximately linear manner, demonstrating that the conductivity waveform in the elastic tube model (see solid line in Fig. 2) is similar to the radius waveform (see dashed line in Fig. 1). However, the conductivity in the rigid tube model (see asterisk in Fig. 3) exhibits a short straight

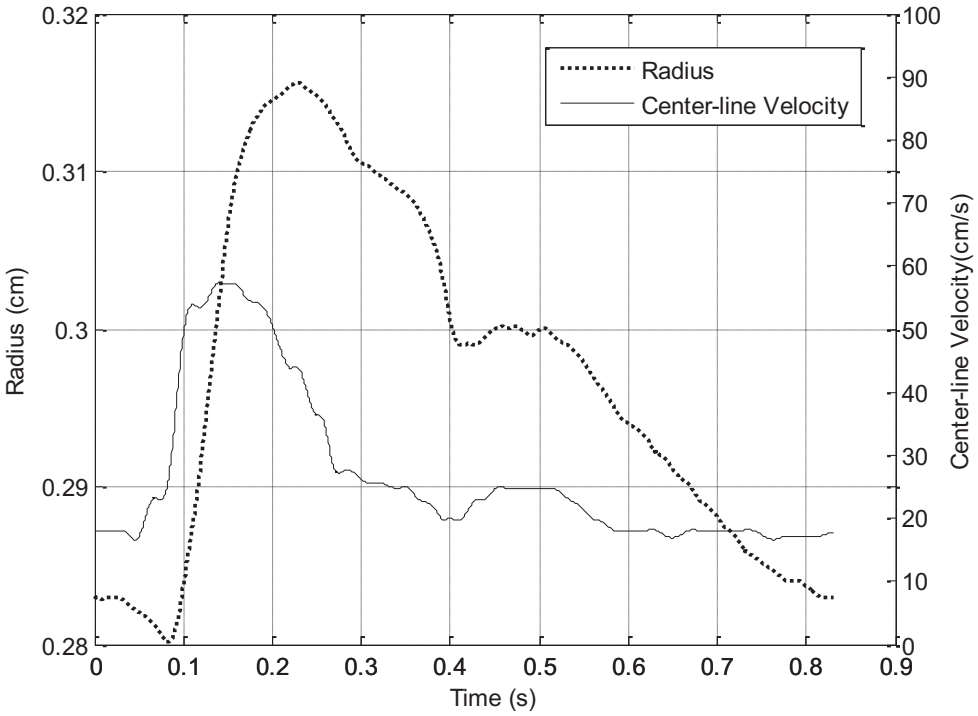

Fig. 1. Instantaneously measured waveforms using an ultrasound Doppler instrument. The dashed line shows the measured result of the radius waveform. The solid line shows the measured result of the center-line velocity waveform.

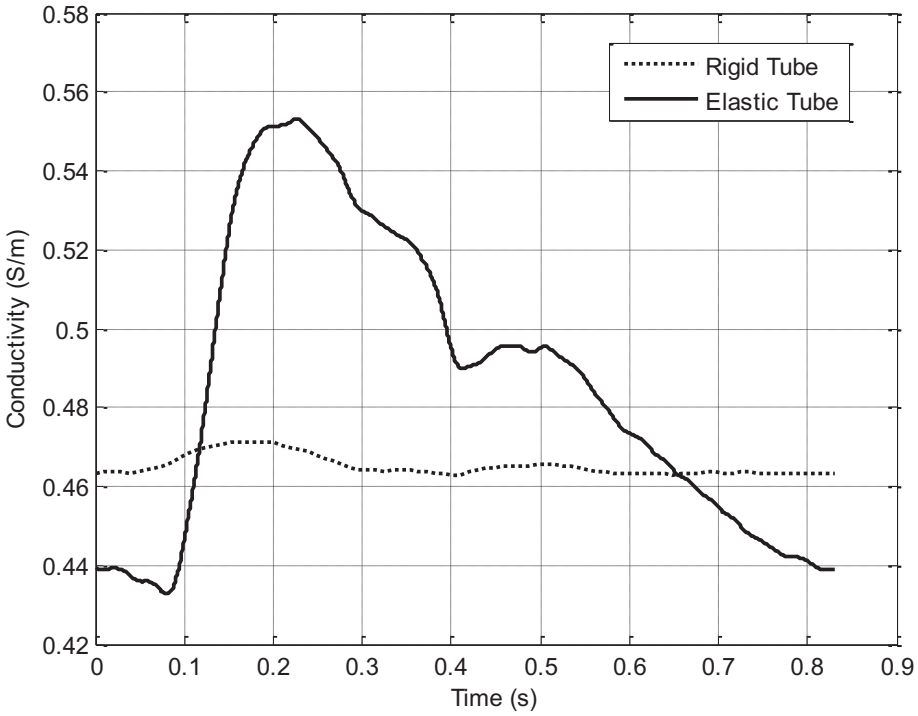

Fig. 2. Simulated conductivity of pulsatile blood flow in a human common carotid artery in the elastic tube model and rigid tube model. The dashed line shows the results from the rigid tube model. The solid line exhibits the results from the elastic tube model.

segment perpendicular to the horizontal axis (radius) because the radius remains constant over one cardiac cycle, demonstrating that the pulsatile flow velocity will be another influencing factor in addition to changes in the radius (wall motion).

To clarify this point, the conductivity versus center-line velocity plot over one cardiac cycle by the rigid and elastic tube models are shown in Fig. 4.

As shown in Fig. 4, a significant discrepancy in the simulation results is exhibited by the two models (see also Fig. 2). For the elastic tube model, the conductivity gradually increases from 0.43 S/m to 0.46 S/m as the center-line velocity increases from 17 cm/s to 54 cm/s during the systolic acceleration phase; however, the conductivity gradually decreases from 0.55 S/m to 0.53 S/m as the center-line velocity decreases from 55 cm/s to 27 cm/s

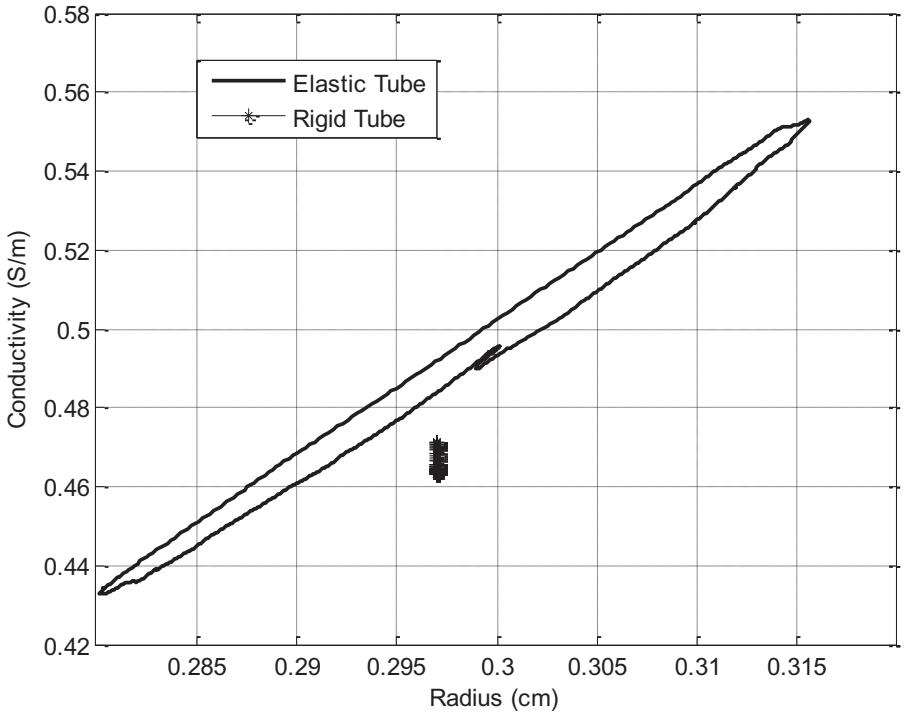

Fig. 3. Conductivity versus radius over one cardiac cycle. The circle shows the results from the rigid tube model. The solid line exhibits the results from the elastic tube model.

during the diastolic deceleration phase. The abrupt variation in conductivity occurs as the center-line velocity begins to change between the acceleration phase and deceleration phase. For the rigid tube model, the conductivity against the center-line velocity also exhibits a similar hysteretic behavior (Fig. 4(b)), except that the pulsating amplitude of the conductivity is much smaller than that in the elastic tube model (see Fig. 4(a)).

3.2. Effect of wall motion variation on the conductivity

To evaluate the effect of wall motion variation on the conductivity, three plots of the conductivity are given for 0 and ±20% of the pulsating amplitude of the radius, as shown in Fig. 5.

As is shown in Fig. 5(a), the pulsating amplitude of the conductivity exhibits significant changes as the wall pulsation increases or decreases by 20%. To further quantitatively understand this point, Fig. 5(b) shows the maximum, mean and minimum values of the conductivity over one cardiac cycle changes with change in the pulsating amplitude of radius (ranging from −20% to 20%). It is clearly seen from Fig. 5(b) that as the pulsating amplitude of the radius increases from −20% to 20%, the maximum of the conductivity increases, while its minimum decreases; however, the mean value of the conductivity almost remains constant.

3.3. Effect of variation in velocity waveform on the conductivity

Analogously to the case of wall motion, Fig. 6 shows the influence of conductivity in the elastic tube model induced by the center-line velocity change.

As is shown in Fig. 6(a), although the pulsating amplitude of the center-line velocity changes from −20% to +20%, the conductivity remains almost unchanged. This means that the conductivity in the elastic tube model is not sensitive to the change of the center-line velocity. The same conclusion can also be attained from Fig. 6(b), where the maximum, mean and minimum of the conductivity remain unchanged, while the pulsating amplitude of the center-line velocity changes from −20% to 20%.

4. Discussion

Although a number of studies have been documented to investigate the effect of steady or pulsatile blood flow on conductivity [6,8,11,13,18,22], the influence of the elastic deformation of the blood vessel wall on conductivity has not been found in the literature. In this paper, an elastic tube model is proposed to explore the effect of wall motion on the conductivity of arterial pulsatile blood flow. Further, numerical simulation studies are conducted to compare the conductivity divergence between the elastic tube model and rigid tube model. In addition to the axial center-line velocity variable, we introduce the arterial radius as the second variable in the elastic model. Numerical simulations are performed to investigate which is the prominent player in influencing the conductivity.

The conductivity of pulsatile blood flow in arteries may be influenced by two factors: (i) RBC orientation and deformation [8,22]; (ii) arterial radius [11,13,23]. However, in the previous investigations of the rigid tube model [11,13,24], the arterial radii were assumed to be constant values; thus, blood-flow-induced RBC orientation and deformation were the sole determinants affecting the conductivity. This is not in accordance with the physiological case because the arterial radius is dynamically changing as a result of the wall elasticity of arteries. The pulsating amplitude of the conductivity will become much larger than that in the rigid tube model (see Figs. 2–4) when wall motion is considered in the elastic tube model. This result/finding suggests that the pipe diameter changes and the blood flow velocity also play a vital role in inducing the conductivity discrepancy between the rigid tube model and elastic tube model, indicating that the rigid tube model [9–11] will cause significant errors in calculating the conductivity of arterial pulsatile blood flow.

Blood flow velocity and wall motion are two important factors affecting the conductivity. Our simulation results (see Figs. 5 and 6) suggest that the variation in wall motion may significantly influence the conductivity (Fig. 5), while the change in center-line velocity induces an insignificant effect (Fig. 6), demonstrating that blood conductivity is much more affected by the diameter rather

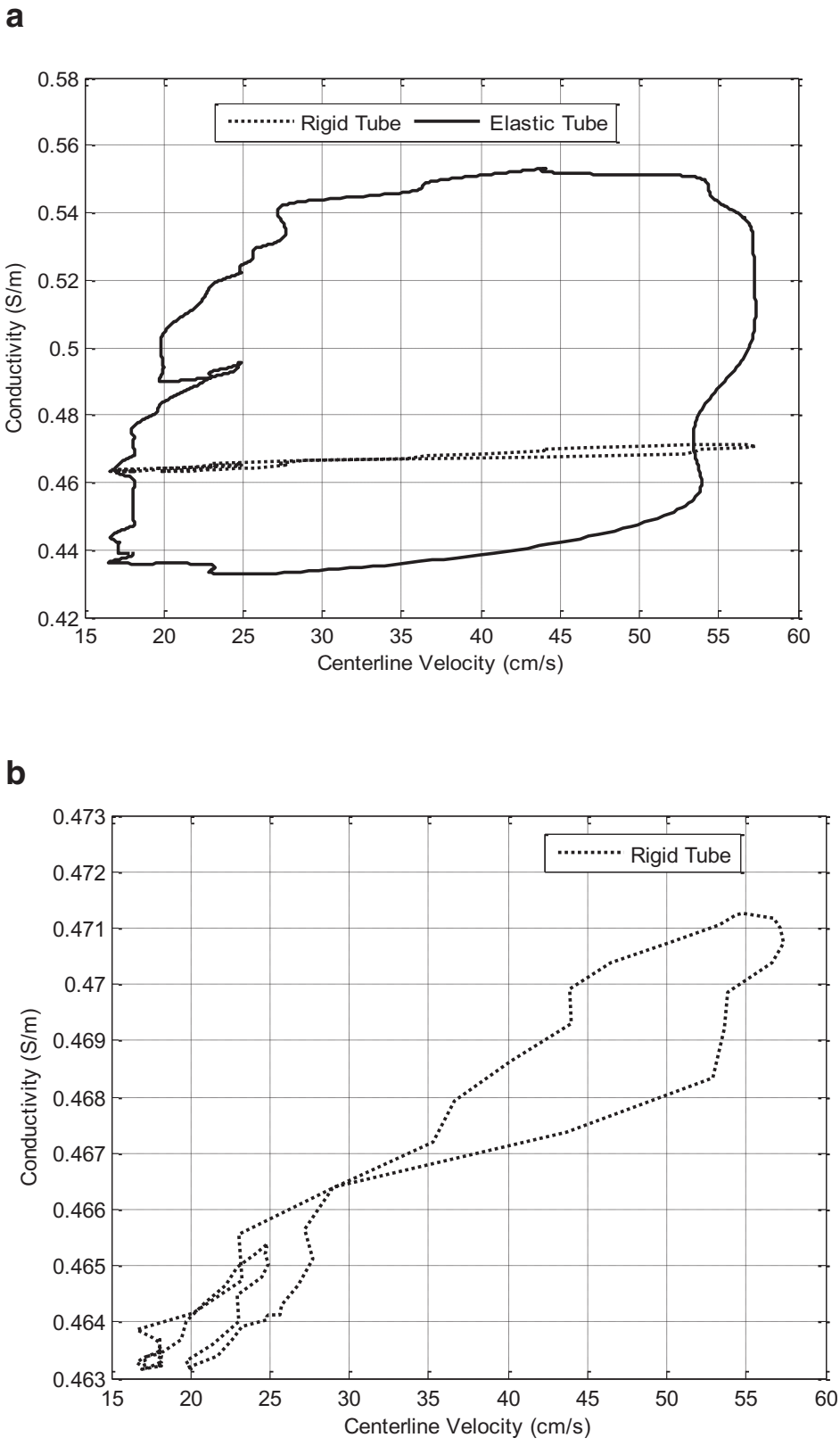

Fig. 4. Conductivity versus center-line velocity over one cardiac cycle. (a) The dashed line shows the results from the rigid tube model. The solid line exhibits the results from the elastic tube model; (b) conductivity versus center-line velocity by the rigid tube model with an independent coordinate.

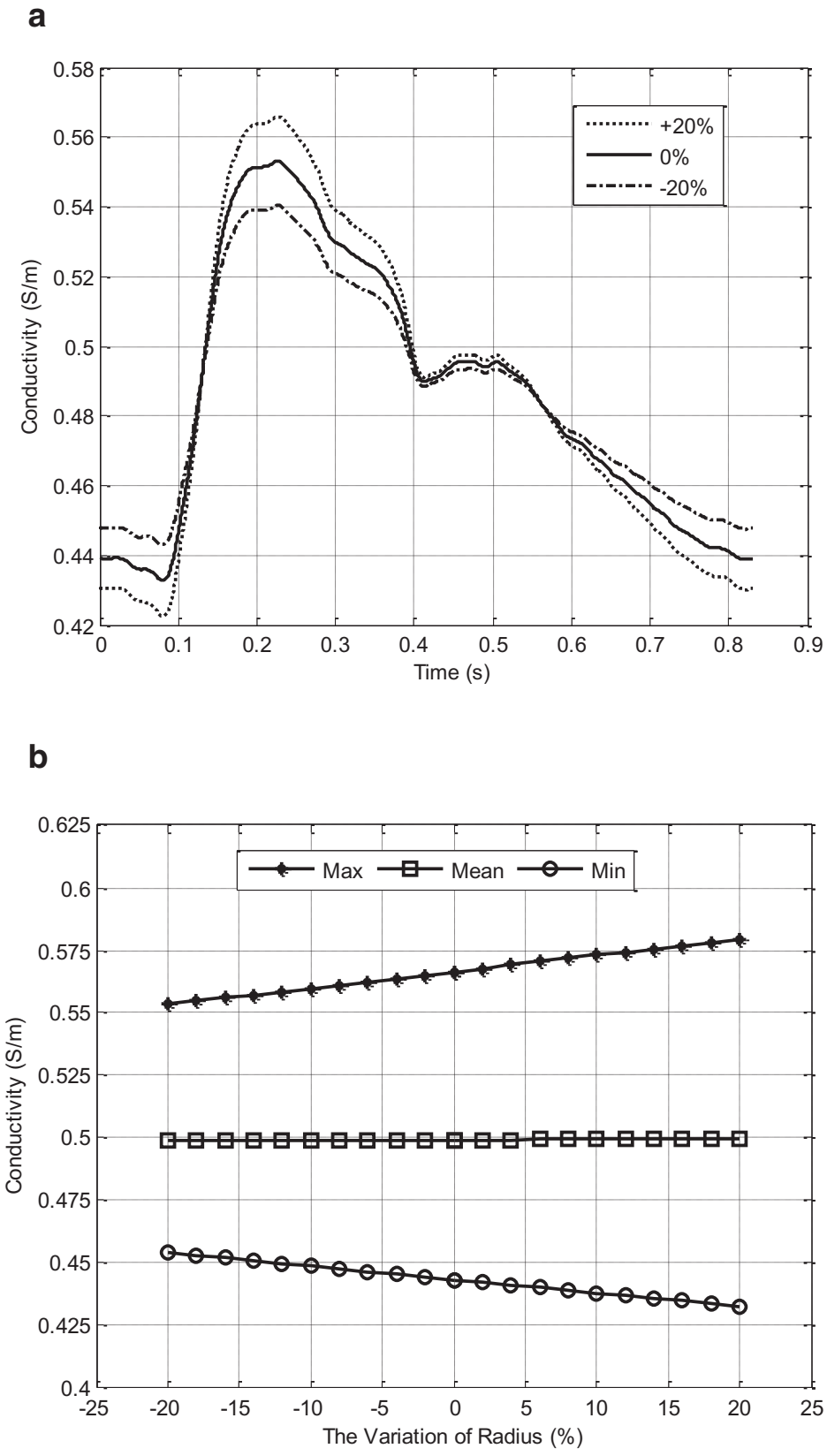

Fig. 5. Effect of variation in wall motion on the conductivity. (a) Conductivity versus time; (b) maximum, mean, and minimum of conductivity versus variation in wall motion.

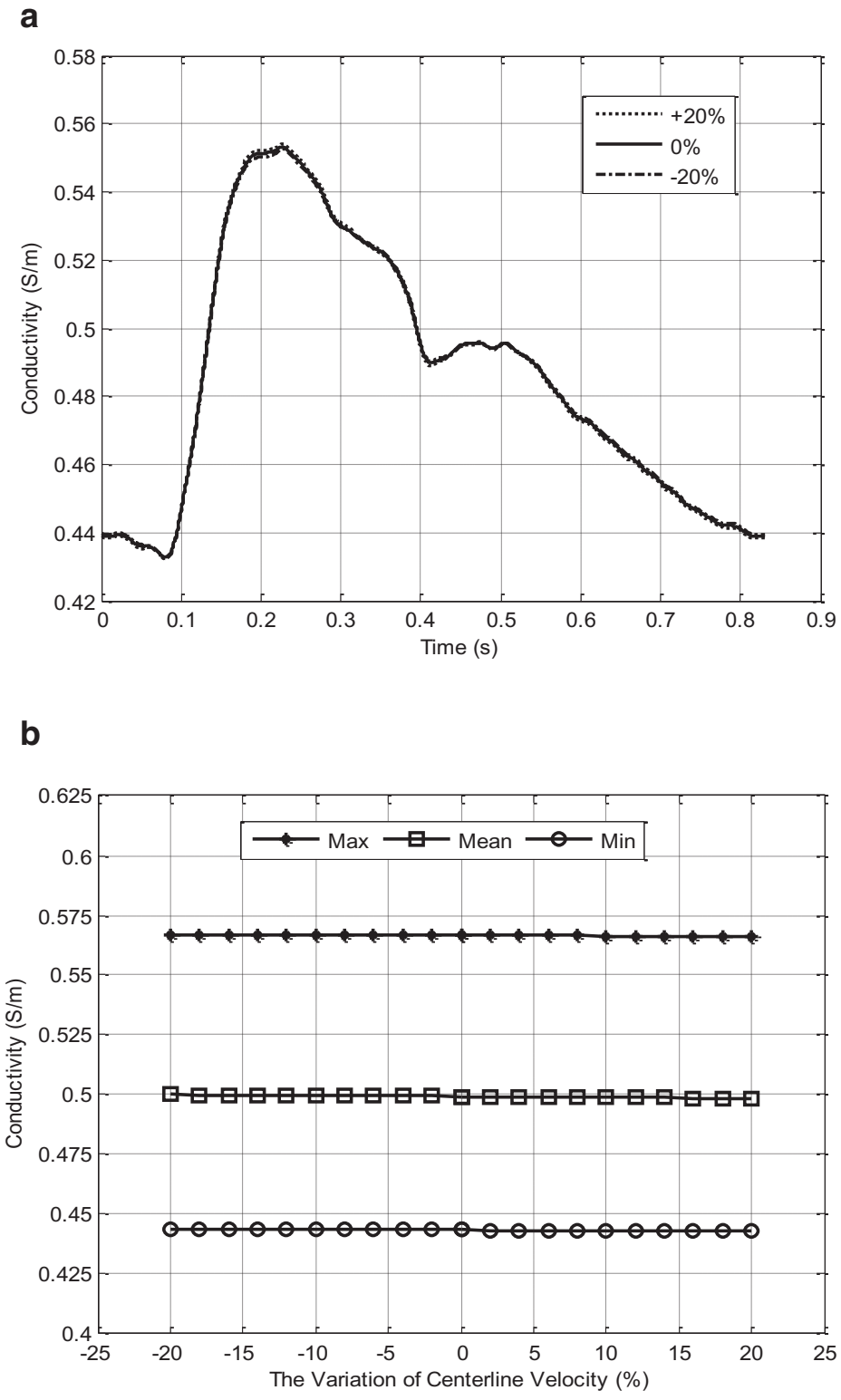

Fig. 6. Effect of variation in velocity waveform on conductivity. (a) Conductivity versus time; (b) maximum, mean and minimum of the conductivity versus variation in center-line velocity.

than the center-line velocity. It can be seen from Eq. (16) that the blood conductivity $\sigma_{bl}(t)$ is determined by the radial conductivity $\sigma_c(y, t)$ that is primarily influenced by the shear stress (see Eqs. (17)–(27)). Therefore, it can be safely concluded that the wall motion affects the blood conductivity by regulating the blood-flow-induced shear stress; this can be verified by the difference between shear stress waveforms in the rigid tube model and in the elastic tube model (see the comparison of wall shear stress in Fig. 7).

The effect of the pulsatile blood flow velocity on the conductivity in the rigid tube has been well documented in the literature [9–11]. Gaw et al. [11] reported that there is a time delay between

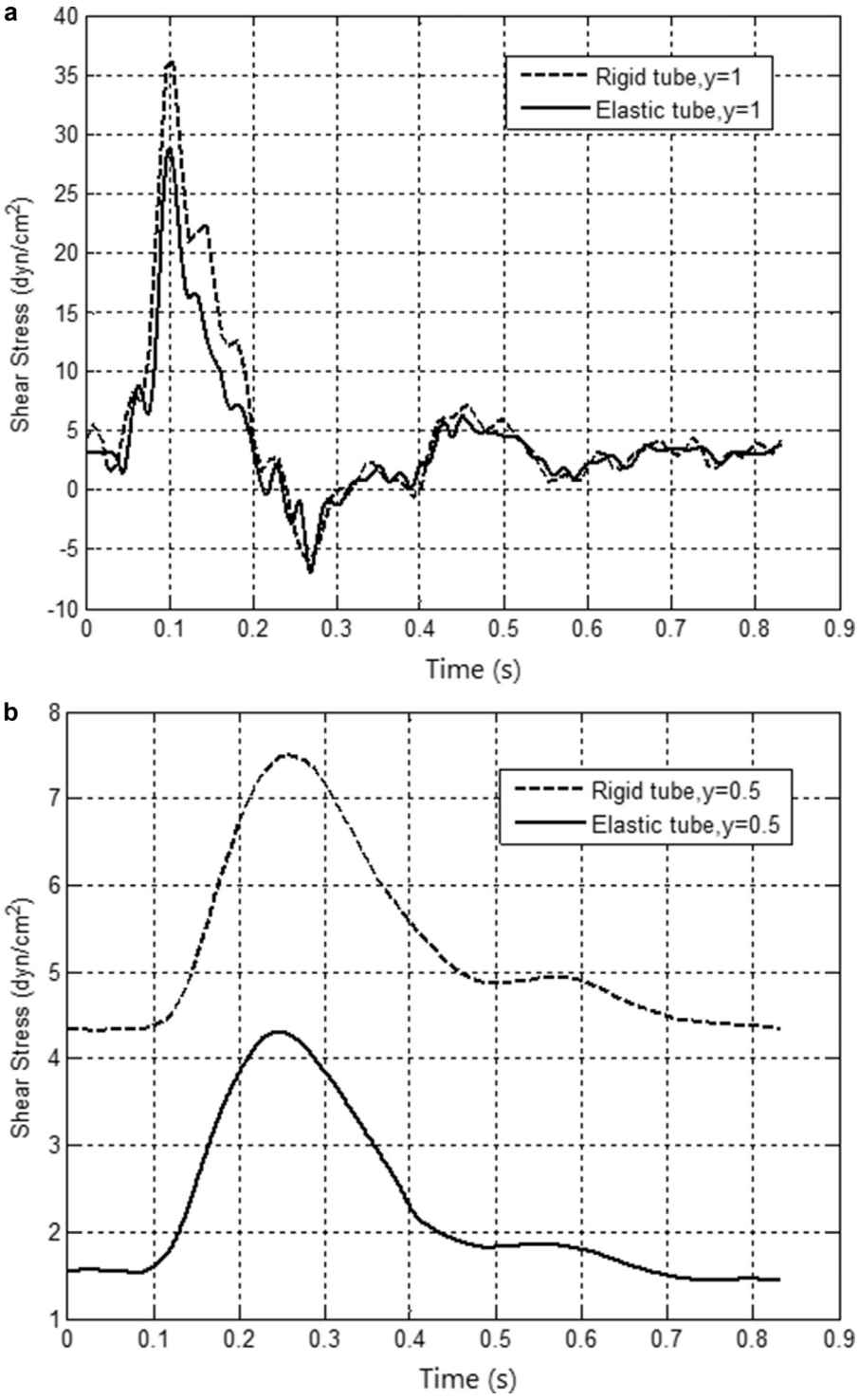

Fig. 7. The shear stress waveform over one cycle from the elastic tube model and from the rigid tube model. The dashed line shows the result from the rigid tube model. The solid line exhibits the result from the elastic tube model. (a) At the position of $y = 1$; (b) at the position of $y = 0.5$; $y = r/R$ is a relative radial coordinate, r is the radial coordinate and R is the arterial inner radius.

the conductivity response and blood flow stopping, suggesting that RBCs take time to reorient. Our simulation results (see solid line in Fig. 4(a)) also confirm these findings to some extent. It is seen from Fig. 4(a) that no significant changes in conductivity could be observed during most of the time in the acceleration or deceleration phase; a sharp variation in conductivity can only be observed in a short time period. Specifically, the blood flow changes the flow direction from the acceleration phase to the deceleration phase or vice versa. Such hysteretic behavior is interesting and was also found in the literature (see Fig. 4, [11]) in the rigid tube model. However, our simulation results (Fig. 6) in the elastic tube model demonstrate that the variation in center-line blood velocity plays an insignificant effect on the total conductivity of blood.

It is worth noting that this study is only based on theoretical computation. In our future work, an *in vitro* experimental setup is being developed to validate the elastic tube

model and the simulation results. Furthermore, the present study may contribute to developing more accurate *in-vivo* electrical-impedance-based clinical applications.

5. Conclusion

The elastic tube model proposed in this study theoretically shows that conductivity changes are simultaneously determined by both wall motion and center-line blood flow velocity. Wall motion, rather than center-line blood flow velocity, is the primary factor that affects the conductivity of flowing blood in an artery.

Competing interests

None declared.

Funding

This work is, in part, supported by the National Natural Science Foundation of China (NNSFC) under Grant no. 31370948; Liaoning Province Science Fund for Public Interest Research under Grant no. 2014001027.

Ethical approval

Not required.

Acknowledgments

The authors would like to acknowledge Dr. Xiaoling Sun for the insightful advice and Prof Wenyu Liu for English editing.

Supplementary materials

Supplementary material associated with this article can be found, in the online version, at doi:10.1016/j.medengphy.2016.09.013.

References

[1] Bera TK. Bioelectrical impedance methods for noninvasive health monitoring: A review. J Med Eng 2014(2014):1–28.
[2] Berbich L, Bensalah A, Flaud P, Benkirane R. Non-linear analysis of the arterial pulsatile flow: Assessment of a model allowing a non-invasive ultrasonic functional exploration. Med Eng Phys 2001;23(3):175–83.
[3] Bitbol M, Quemada D. Measurement of erythrocyte orientation in flow by spin labeling II – Phenomenological models for erythrocyte orientation rate. Biorheology 1985;22:31–42.
[4] Dutta A, Wang DM, Tarbell JM. Numerical analysis of flow in an elastic artery model. J Biomech Eng 1992;114(1):26–33.
[5] Flaud P, Bensalah A. Indirect instantaneous velocity profiles and wall shear rate measurements in arteries: A centre-line velocity method applied to non-Newtonians fluids. In: Power H, Hart BT, editors. Computer simulations in biomedicine. Computational Mechanics Publications; 1995. p. 191–9.
[6] Frewer RA. The electrical conductivity of flowing blood. Biomed Eng 1975;9(12):552–5.
[7] Fricke H. A mathematical treatment of the electric conductivity and capacity of disperse systems I. The electric conductivity of a suspension of homogeneous spheroids. Phys Rev 1924;24(5):575–87.
[8] Fujii M, Nakajima K, Sakamoto K, Kanai H. Orientation and deformation of erythrocytes in flowing blood. Ann N Y Acad Sci 1999;873(1):245–61.
[9] Gaw RL, Cornish BH, Thomas BJ. Comparison of a theoretical impedance model with experimental measurements of pulsatile blood flow. In: Proceedings of the thirteenth international conference on electrical bioimpedance and the eighth conference on electrical impedance tomography. Springer Berlin Heidelberg; 2007. p. 32–5.
[10] Gaw RL, Cornish BH, Thomas BJ. The electrical impedance of pulsatile blood flowing through rigid tubes: An experimental investigation. IFMBE Proc 2006;17(2):73–6.
[11] Gaw RL, Cornish BH, Thomas BJ. The electrical impedance of pulsatile blood flowing through rigid tubes: A theoretical investigation. IEEE Trans Biomed Eng 2008;55(2):721–7.
[12] Heffernan KS, Jae SY, Wilund KR, Woods JA, Fernhall B. Racial differences in central blood pressure and vascular function in young men. Am J Physiol Heart Circ Physiol 2008;295(6):H2380–7.
[13] Hoetink AE, Faes TJC, Visser KR, Heethaar RM. On the flow dependency of the electrical conductivity of blood. IEEE Trans Biomed Eng 2004;51(7):1251–1261.
[14] Jayaraman G, Sarkar A. Nonlinear analysis of arterial blood flow – Steady streaming effect. Nonlinear Anal 2005;63(5–7):880–90.
[15] Ling SC, Atabek HB. Nonlinear analysis of pulsatile flow in arteries. J Fluid Mech 1972;55:493–511.
[16] Liu HB, Yuan WX, Qin KR, Hou J. Acute effect of cycling intervention on carotid arterial hemodynamics: basketball athletes versus sedentary controls. Biomed Eng Online 2015;14(Suppl 1):S17.
[17] Ninomiya M, Fujii M, Niwa M. Physical properties of flowing blood. Biorheology 1988;25:319–28.
[18] Sakamoto K, Kanai H. Electrical characteristics of flowing blood. Iyō Denshi to SeitaiKōgaku, Jpn J Med Electron Biol Eng 1978(1):45–52.
[19] Sodolski T, Kutarski A. Impedance cardiography: A valuable method of evaluating haemodynamic parameters. Cardiol J 2007;14(2):115–26.
[20] Sugawara M, Niki K, Furuhata H, Ohnishi S, Suzuki S. Relationship between the pressure and diameter of the carotid artery in humans. Heart Vessel 2000;15(1):49–51.
[21] Summers RL, Shoemaker WC, W Franklin P, Ander DS, Coleman TG. Bench to bedside: electrophysiologic and clinical principles of noninvasive hemodynamic monitoring using impedance cardiography. Acad Emerg Med 2003;10(6):669–80.
[22] Visser KR. Electric conductivity of stationary and flowing human blood at low frequencies. Med Biol Eng Comput 1992;30(6):636–40.
[23] Visser KR. Electric properties of flowing blood and impedance cardiography. Ann Biomed Eng 1989;17:463–73.
[24] Visser KR, Lamberts R, Korsten HHM, Zijlstra WG. Observations on blood flow related electrical impedance changes in rigid tubes. Pflüg Archiv Eur J Physiol 1976;366(2-3):289–91.
[25] Wang DM, Tarbell JM. Nonlinear analysis of flow in an elastic tube (artery): Steady streaming effects. J Fluid Mech 1992;239(1):341–58.
[26] Wang DM, Tarbell JM. Non-linear analysis of oscillatory flow, with a non-zero mean, in an elastic tube (artery). J Biomech Eng 1995;117(1):127–35.
[27] Webster JG, Clark JW. Medical instrumentation: Application and design. J. Wiley; 2010.
[28] Womersley JR. Oscillatory flow in arteries: The constrained elastic tube as a model of arterial flow and pulse transmission. Phys Med Biol 1957;2(2):178–87.
[29] Womersley JR. An Elastic Tube Theory on Pulse Transmission and Oscillatory Flow in Mammalian Arteries. Wright Air Development Center. WADC Tech. Rep. 1957.